Use of ArcGIS to extract river geometry as an input to HECRAS model and inundation mapping for the Lower Colorado River (LCR), Texas from Highway 183 to Bastrop.

Muhammad Rezaul Haider (A 02196036).

Date of Submission: 12.03.2016.

Email: rezaulwre@gmail.com

Course No.: CEE 6440, Fall 2016.

Submitted to:

Dr. David G Tarboton, Professor, Utah State University.

Introduction:

Floods are costly natural disasters causing fatalities, damages to life, property, communications, transportation, and critical infrastructures (Kalyanapu et al., 2010). Floodplain modeling is a relatively new and applied method in river engineering discipline and is essential for prediction of flood hazards, and the purpose of managing and performing all river training practices (Salimi et al. 2008). For this project I explored integrating of HEC-RAS (US Army Corps of Engineers, 2016) and ArcGIS to prepare inundation map (inundation extents and depths) within the floodplain of the Lower Colorado River (LCR), Texas for floods of different return periods.

This report begins with a statement of the project objectives, an overview of the related works found in literature, a brief description of the study area, sources of the data used, and the methodology applied for the current analysis. Next, the results obtained from HEC GeoRAS (a GIS extension) (US Army Corps of Engineers, 2016), and HECRAS model are presented. Finally the inundation maps produced through post processing of model results and conclusion are presented.

Objectives:

The specific objectives of this project are to:

- Extract river cross section from high resolution DEM using ArcGIS.
- Prepare inundation map for floods of different return periods.

Literature Review:

Sanders B.F. (2007) developed flood inundation map using on-line digital elevation models (DEMs). They examined the sensitivity of flood model predictions to DEM type, resolution and accuracy. Merwade et al. (2008) explored GIS techniques for creating continuous river bathymetry from linear cross-sections, and integrating this bathymetry with surrounding topography to produce a coherent river terrain model. This terrain model was then used for hydrodynamic modeling and flood inundation mapping for three different types of river reaches in USA. Several studies also explored the prospects of the methodology of flood mapping based on satellite images and surface elevation data. For example, Sanyal and Lu, 2004 applied GIS and satellite images for flood risk management and concluded that the availability of remote sensing data for flood extent delineation could be more efficient in developing countries because of lacking observed data and cost involved to collect those data.

Study area:

The study area covers an approximately 90 km reach of the LCR, bounded upstream by the USGS gage # 08158000 below Hwy 183 (or just Hwy 183) and downstream by the USGS gage # 08159200 at Bastrop (or just Bastrop) (Figure 1). The land use distribution within the LCR catchment area consists mainly of agricultural, residential, and urban areas (Briody et al. 2016). The LCR is subject to frequent flooding. An example flood hydrograph for the LCR for the period of 2015 (Oct-Nov) is shown in Figure 2.
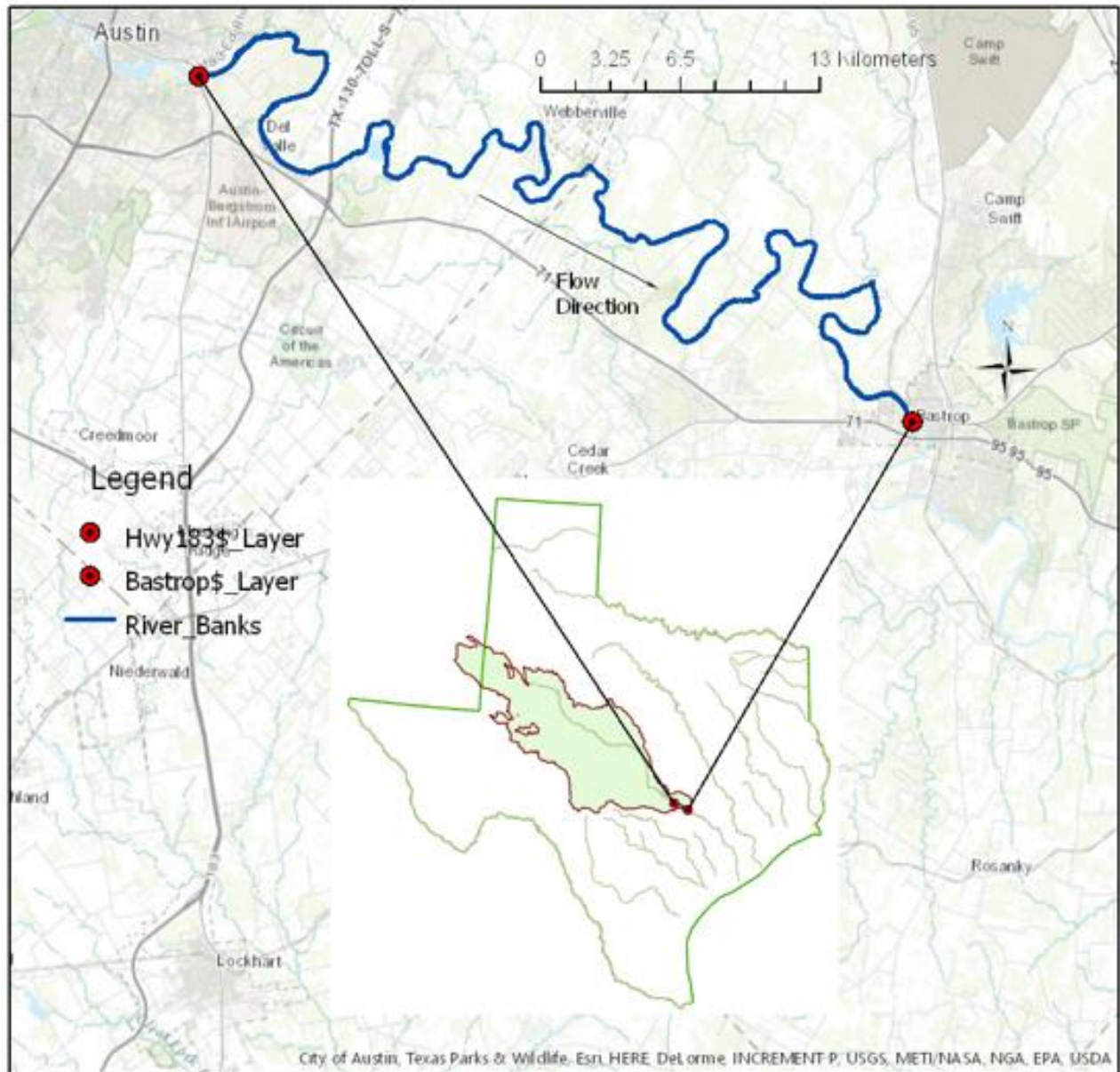
Figure 1: Map of the study reach along the Colorado River bounded by USGS gage # 08158000 at Hwy 183 and # 08159200 at Bastrop.

Data Collection:

Streamflow data for two gages at the upper and lower boundaries of the study area were collected form USGS website. USGS elevation data at a resolution of 1/3 arc-second (approximately 10 meters) covering the whole basin was downloaded from The National Map Viewer (USGS, 2016). Land cover data was downloaded by using the ESRI online service (URL: http://landscape2.arcgis.com/arcgis/).
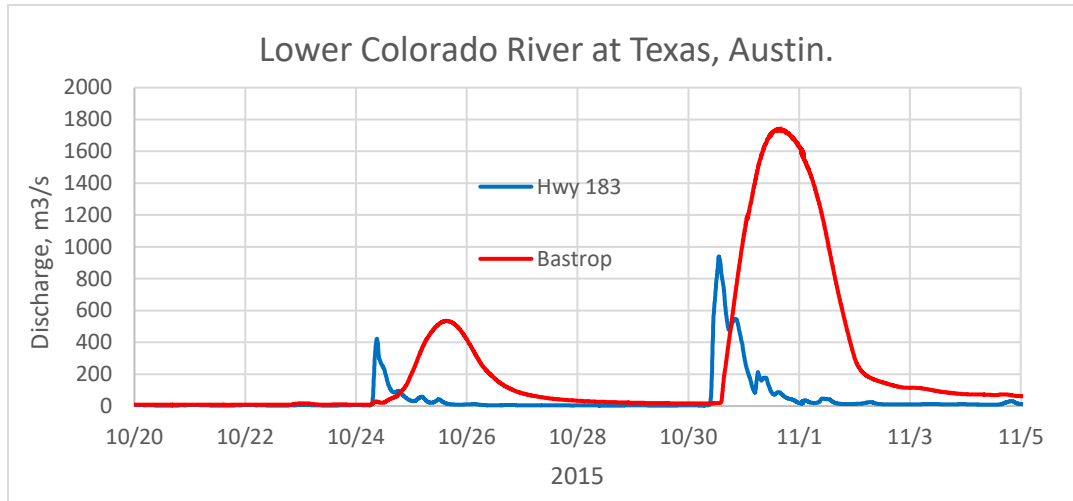
Figure 2: USGS observed discharge for the LCR at the boundaries of the study area.

Methodology:

Catchment delineation and Digital Elevation Model (DEM): The LCR basin (Figure 1) with respect to USGS gage at Bastrop has been delineated by using online Watershed Delineation of ArcGIS Pro. A total of 30 tiles covering the basin were merged together by running the "Mosaic to New Raster" tool of ArcGIS Pro to from a single DEM for the whole basin. The USGS elevation data comes with the geographic coordinate system "GCS North American 1983". A 1000 m buffer was created around the basin by using the "Buffer" tool. The DEM was extracted only for the basin (with buffer) area by using the "Extract by Mask" tool. The extracted DEM has then been projected to Albers Equal Area Conic Projection.

Extraction of cross-sections using HEC-GeoRAS: HEC-GeoRAS 10.2 (the last version tested by USACE) toolbar was loaded into ArcGIS 10.2 (the latest version that HEC-GeoRAS is compatible with) by customizing the toolbars. The RAS Geometry menu contains functions for pre-processing of GIS data for input to HEC-RAS. The RAS Mapping menu contains functions for post-processing of HEC-RAS results to produce flood inundation map. In HEC-GeoRAS, each attribute is stored in a separate feature class called as RAS Layer. Empty GIS layers was created using the RAS Geometry menu on the HEC-GeoRAS toolbar. For convenience, all the layers was created by a single command (Create RAS Layers→All) rather than creating them individually. Thus HEC-GeoRAS creates a geodatabase in the same folder where the map document is saved.

Creating banklines, centerline and flowpaths: The edges of water in Google Earth image was digitized and saved as a KMZ files. These files was imported in ArcGIS using the "KML to Layer" tool. This created geodatabases with the water edges as polylines. These polylines was converted into features. The new shape files were merged into a single layer using the "Merge" tool. The centerline was created using the "Collapse Dual Lines to Centerline" tool. The flowpath lines were used to determine the downstream reach lengths between cross-sections in the main channel and over bank areas. The center line created by merging the river banks were assigned as the centerline in flowpaths layer.

4
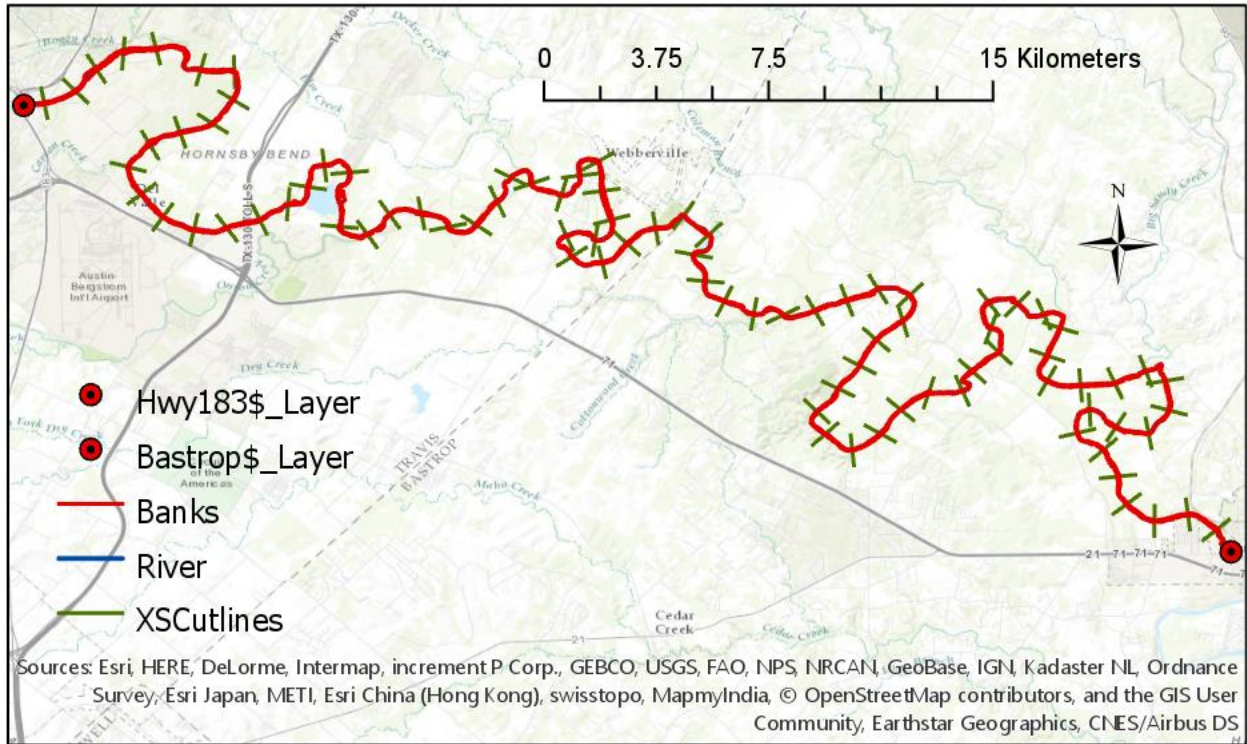
Figure 3: Geometry created in ArcMap using HEC-GeoRAS tools.

Creating cross section cutlines (or XSCutlines): Creating adequate number of cross-sections to produce a good representation of channel bed and floodplain is important (Merwade, 2016). Cross-section cutlines (Figure 3), each of length 1 km, were created by starting editing in XSCutlines feature class. Once created, the XScutlines were assigned HydroIDs (Figure 4), which were really helpful for debugging before entering the geometry into HECRAS. All the layers were projected to NAD83 Albers Equal Area Conic Projection.

Shape *	OID *	Shape_Length	HydroID	Station	River	Reach	LeftBank	RightBank	LLength	ChLength	RLength
Polyline	1	999.999964	8	1000	LCR	Lower	0.45677	0.53716	0	1000	0
Polyline	2	999.999973	9	2000	LCR	Lower	0.46246	0.54282	0	1000	0
Polyline	3	1000.000052	10	3000	LCR	Lower	0.47046	0.53815	0	1000	0
Polyline	4	1000.000059	11	4000	LCR	Lower	0.46969	0.52659	0	1000	0
Polyline	5	1000.000034	12	5000	LCR	Lower	0.46822	0.53734	0	1000	0
Polyline	6	1000.000082	13	6000	LCR	Lower	0.46762	0.52615	0	1000	0
Polyline	7	1000.000038	14	7000	LCR	Lower	0.47768	0.52538	0	1000	0
Polyline	8	1000.000004	15	8000	LCR	Lower	0.48546	0.52225	0	1000	0

Figure 4: Snap shot of XScutlines attribute table extracted from Arc GIS.

Land cover data processing: Land cover data (USA-NLCD_2006) was added to the GIS map. Then "Extract by Mask tool" under the Spatial Analyst Tool was used to mask the land cover data

within the basin delineated earlier. Land cover map is shown on Figure 5. Majority of the land class on the flood plains in the study reach of the LCR include shrub, agriculture, forest, and a little developed area (Table 1).

Hydraulic modeling in HECRAS and post-processing: The geometry was then imported into HECRAS model. Discharge and normal depth (producing an overall water surface slope of 0.0003) were put as the boundary conditions for the upstream and downstream boundaries of the study reach, respectively. Manning's n values were derived from NLCD 2006 Land Use database. LU – Manning Table was created with HEC-GeoRAS and n values (Kalyanapu et al. 2010) were assigned to each land cover class. Manning n-values were assigned to each cross section by using Extract N-Values tool, referring to the class name attribute in land use dataset and LU – Manning Table.
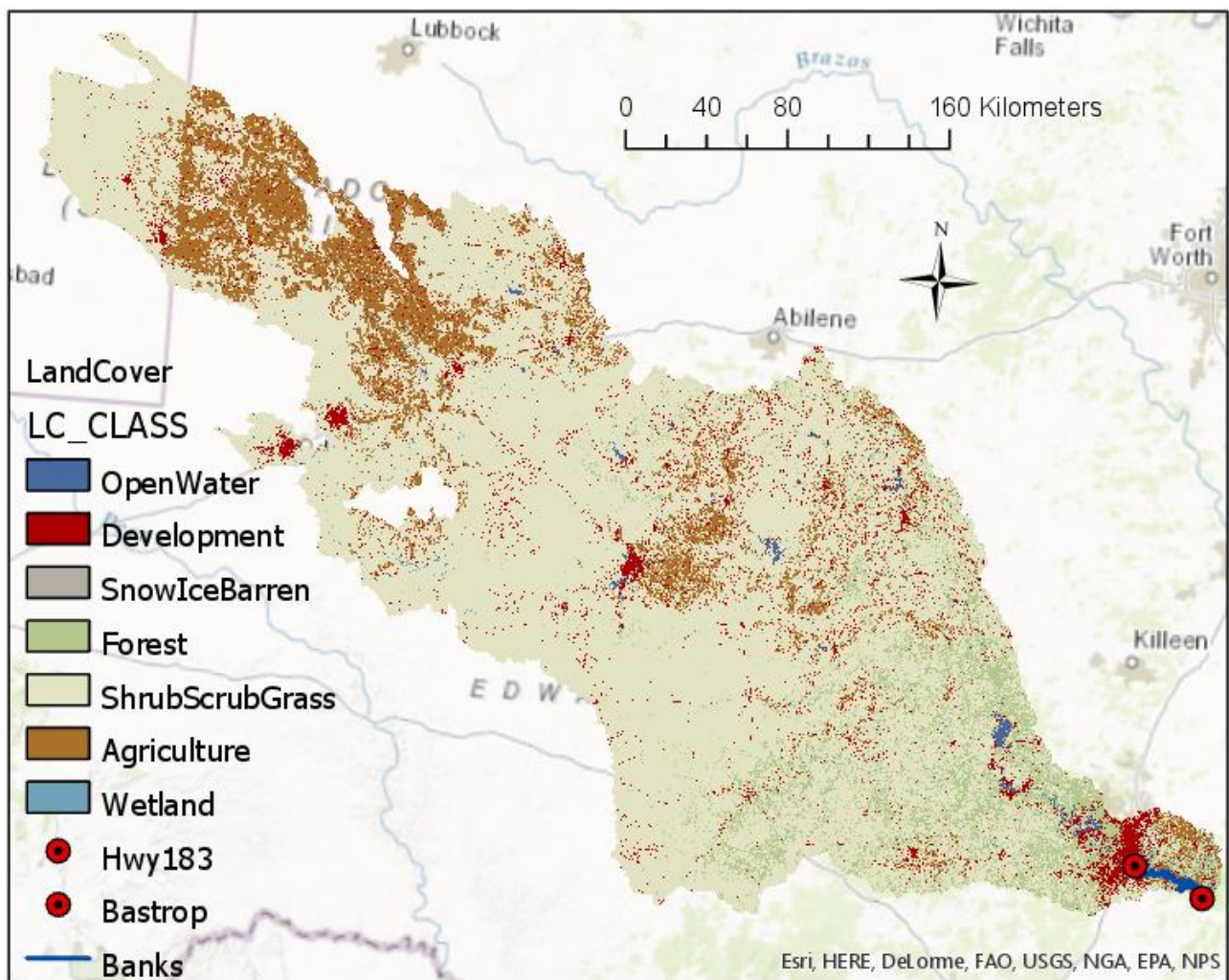
Figure 5: NLCD Land Cover map.

Table 1: Land Cover types.

Land cover type	Areas (km^2)	Percent Area
Open Water	70.15	0.51
Development	672.10	4.91
SnowIceBarren	16.20	0.12
Forest	1069.26	7.81
ShrubScrubGrass	10242.55	74.85
Agriculture	1579.63	11.54
Wetland	34.84	0.25

NLCD 2011 data have been download very recently from USGS website (USGS, 2016). For better estimation of the roughness values in the floodplain, the tiles covering these relatively recent land cover data could be processed in a way similar to that I followed for processing DEM tiles (see DEM processing section above) for the basin.

The historical yearly peak streamflow for USGS gage # 08158000 were calculated from the observed 15-minutes flow data. The flood magnitudes (Table 2) associated with different return periods (2.33, 5, 10, 25, 50, and 100 years) were calculated by putting these yearly peak values into the software package PeakFQ (USGS, 2014). The HEC-RAS model was then simulated for floods of the above return periods with an assumption of steady flow (flow with different return periods).

Table 2: Discharge associated with different return periods.

Return Period (year)	Associated Profile (Plan) in HEC RAS	Scenarios while post-processing in HEC GeoRas (output in Figures 9 and 10)	Discharge (m^3/s)
2.33	Plan 1	inpf1	1580
5.00	Plan 2	inpf2	2568
10.00	Plan 3	inpf3	3641
25.00	Plan 4	inpf4	5413
50.00	Plan 5	inpf5	7092
100.00	Plan 6	inpf6	9125

Inundation mapping: The HEC-RAS output (RAS SDF file) was converted to a TIN file using the tool (RAS Mapping→Inundation Mapping→Water Surface Generation) of HEC Geo RAS. This TIN file forms a bounding polygon created by connecting the endpoints of XS Cut Lines and is the analysis extent for inundation mapping. The TIN file was then converted to Raster. Using Raster calculator of ArcGIS, the underlying DEM terrain layer was subtracted from the water surface raster. The cells with positive values were identified to be flooded and the values (positive ones) were the inundation depth for the respective flooding scenarios / Plan (see Table 2).

Results and Discussion:

A total of 89 cross-sections (at 1 km spacing in 89 km of channel reach) were extracted from HEC-GeoRAS under first objective of this study. Figure 6 shows a cross-section at 15 km upstream of Bastrop.
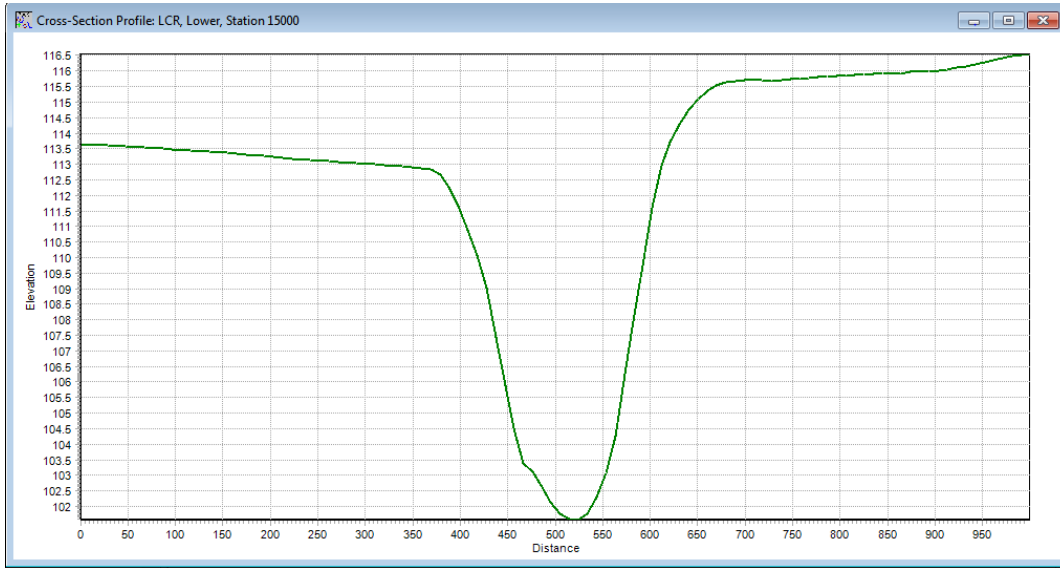
Figure 6: Cross section at 15 km upstream from Bastrop extracted from ArcGIS using HEC GeoRAS extensions.

Figures 7a, 7b, and 7c show the water surface (2-D), 3-D view of water surface, and cross section for a normal flooding condition (return periods 2.33 years), respectively, whereas Figures 8a, 8b, and 8c represent those for a flood of 100 year return period, respectively. From the bed profile (Figure 7a) of the LCR, the overall longitudinal slope was calculated to be 0.0003.
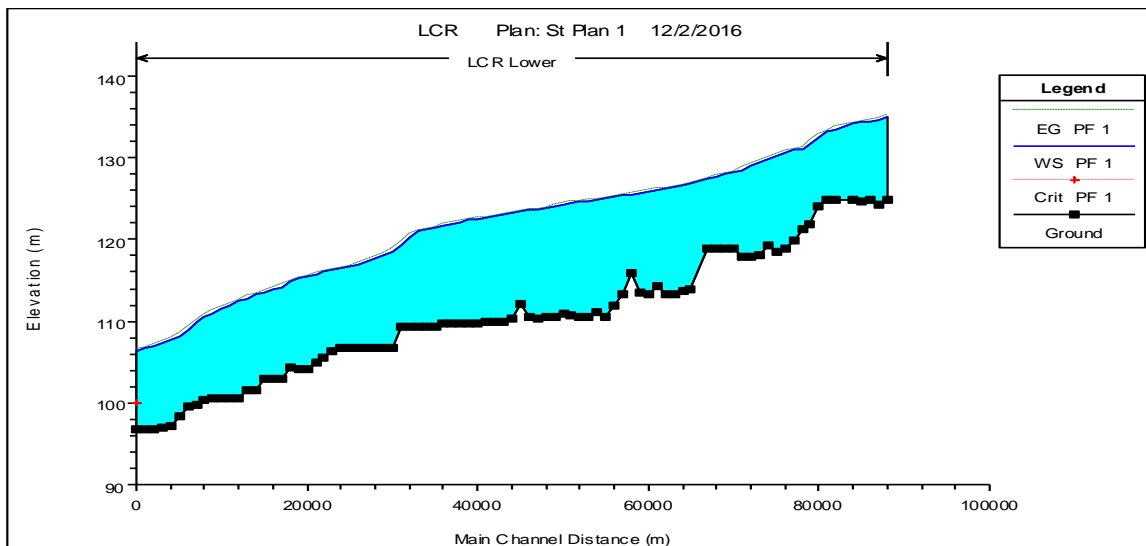
Figure 7a: Water surface profile for a flood of 2.33 years return period as a result of steady flow analysis in HEC-RAS.
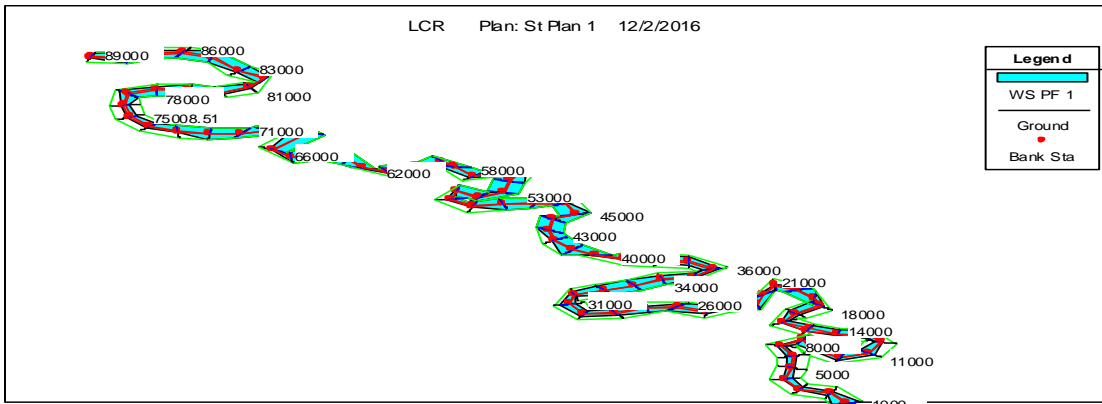
Figure 7b: 3-D view of water surface profile for a flood of 2.33 years return period.
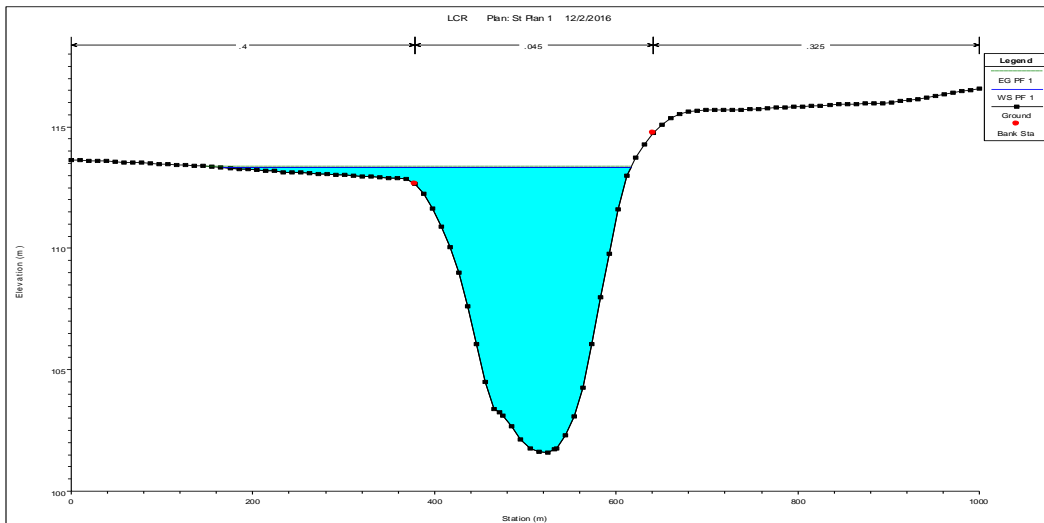
Figure 7c: Cross Section at 15 km upstream of Bastrop for a flood of 2.33 years return period.
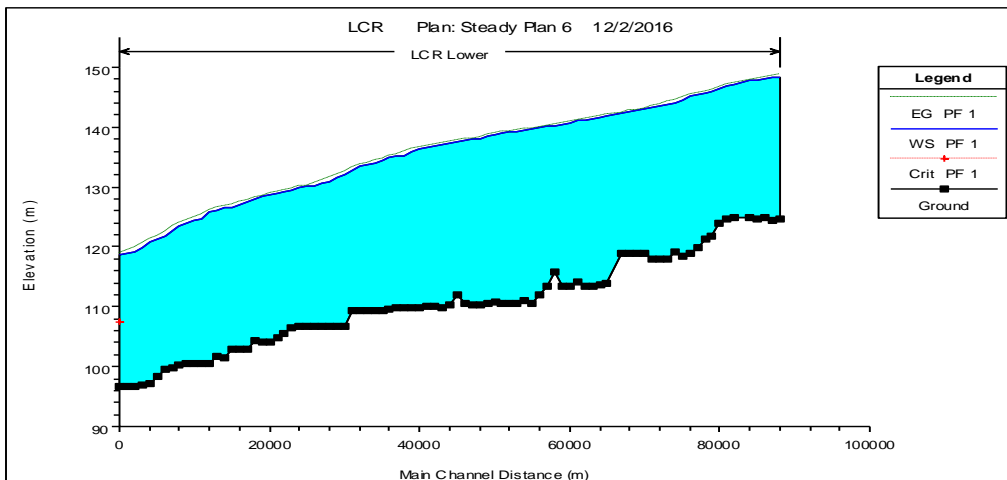
Figure 8a: Water surface profile for a flood of 100 years return period as a result of steady flow analysis in HEC-RAS.

9
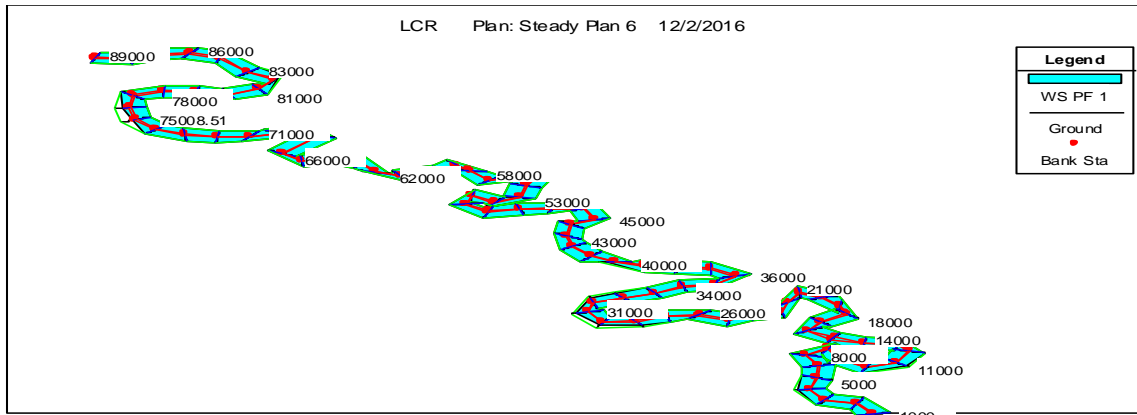
Figure 8b: 3-D view of water surface profile for a flood of 100 years return period.
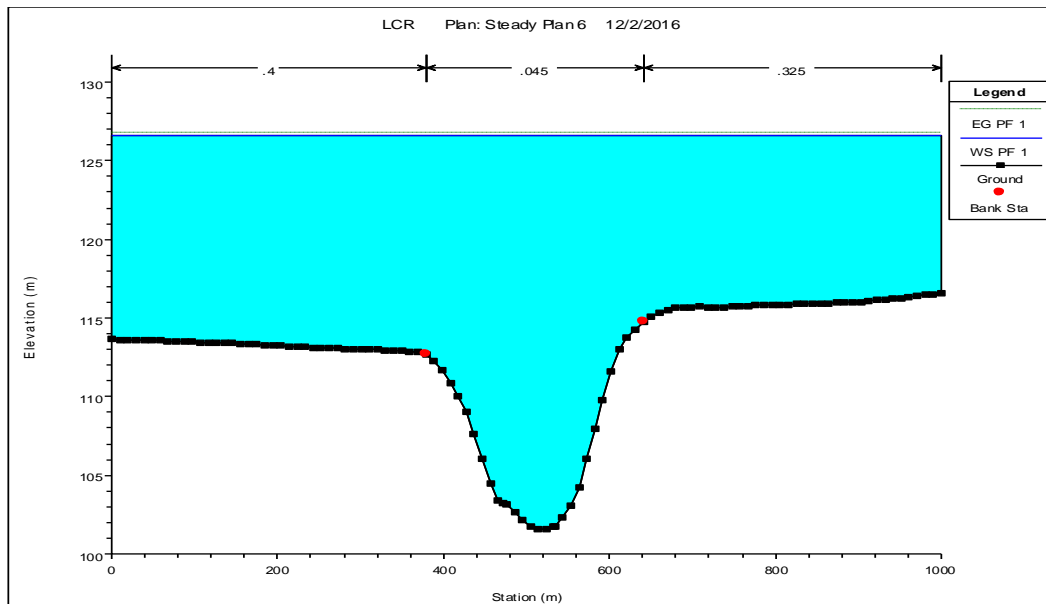
Figure 8c: Cross Section at 15 km upstream of Bastrop for a flood of 100 years return period.

As seen from Figures 7 and 8, the extent of flooding for a return period of 100 years substantially increases (in extent and depth) in compared to that for normal flooding condition. Figures 9 (a, b, and c) and 10 (a, b, and c) show inundation extents of the LCR for floods of different return periods. As is obvious from Figures 9 and 10, the inundation area (with different water depths) increases with floods of increasing return periods, which is also presented in Figure 11. The range of depths were chosen arbitrarily (at three meters interval) with a view to see how the inundation depths change with return periods. The inundation area extends beyond the XScutlines because Raster calculation (see Methodology section) was performed to calculate inundation in the whole floodplain area rather than using "Floodplain Delineation using Raster" tool.
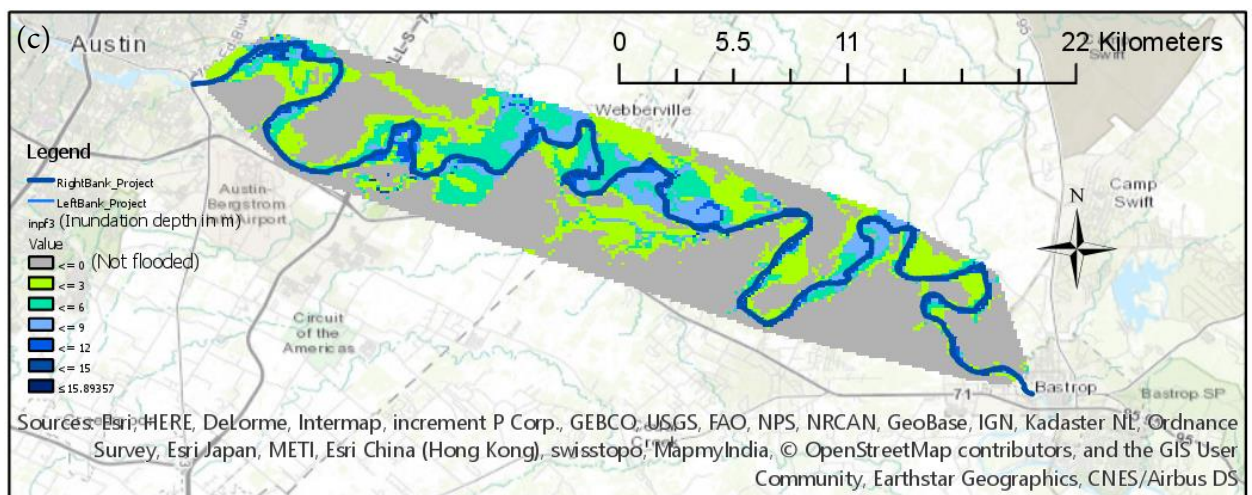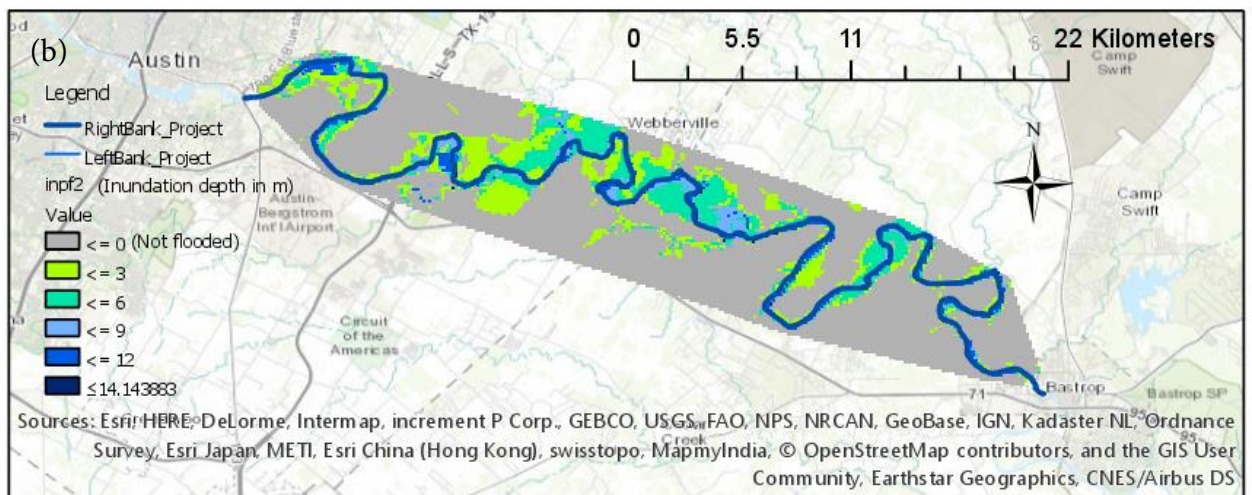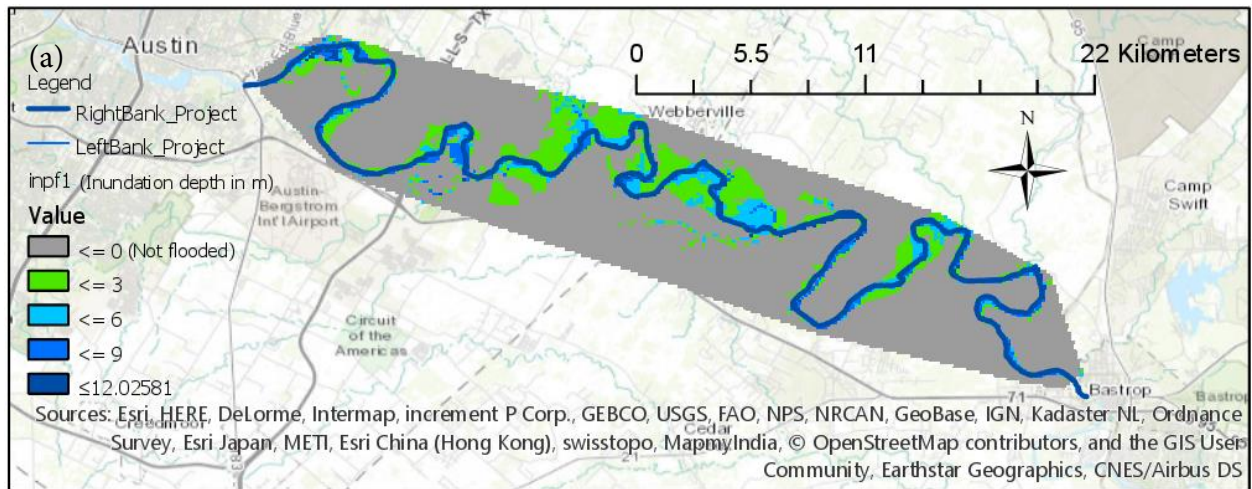
Figure 9: Inundation maps (a, b, and c represent flooding scenarios with return periods of 2.33, 5, and 10 years, respectively).
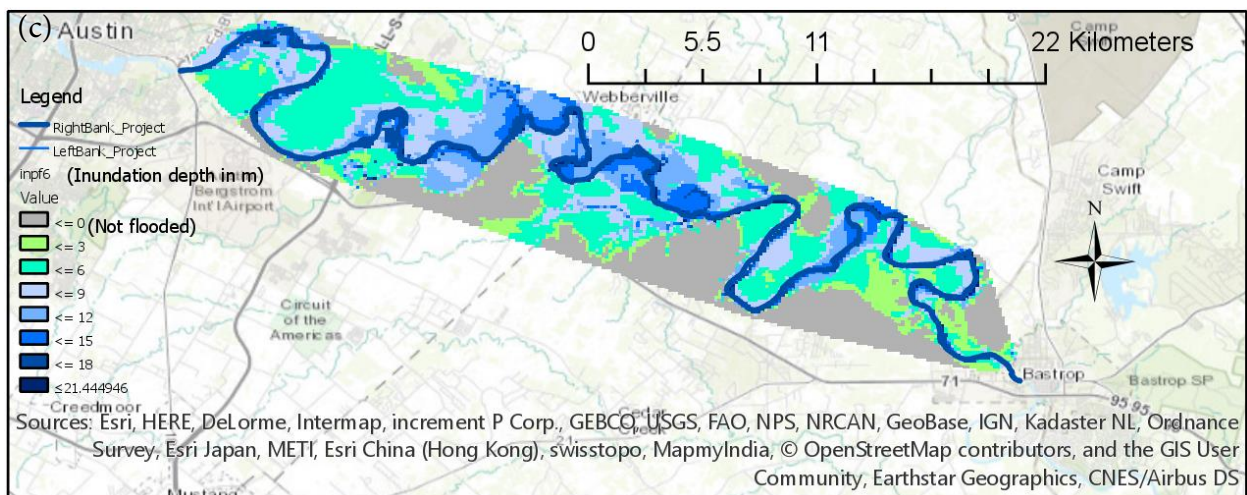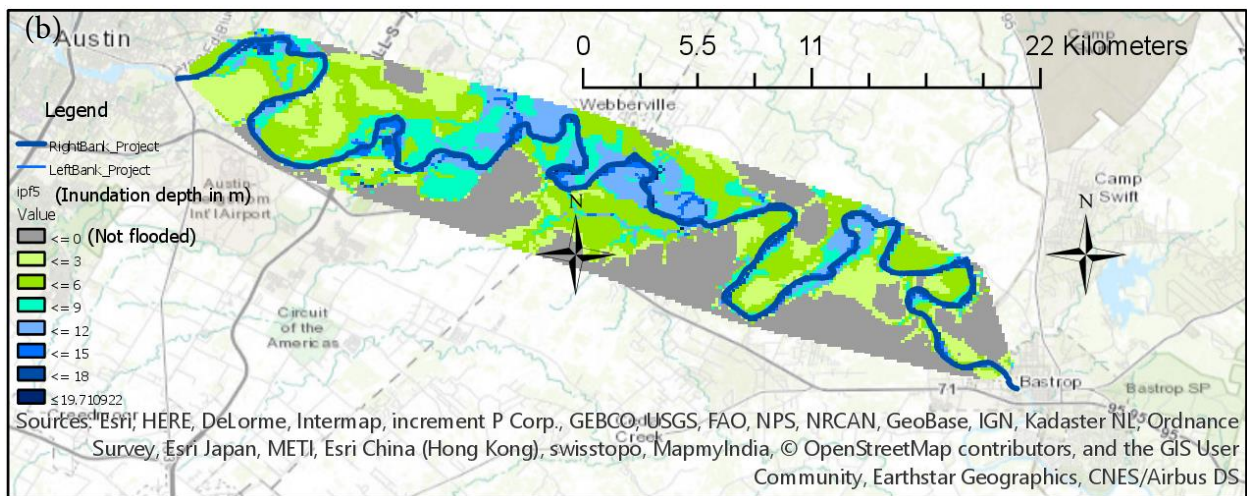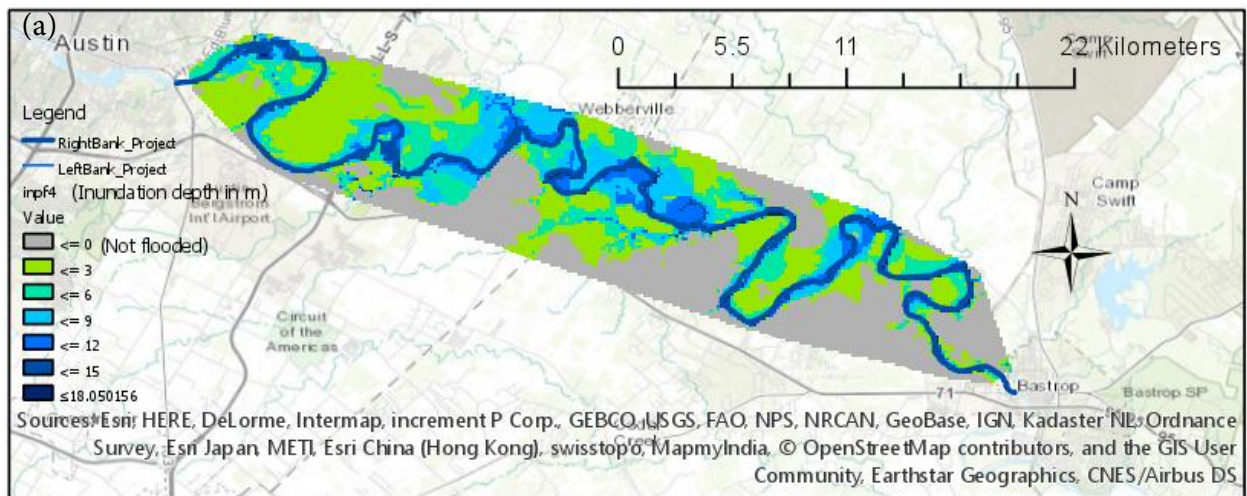
Figure 10: Inundation maps (a, b, and c represent flooding scenarios with return periods of 25, 50, and 100 years, respectively).
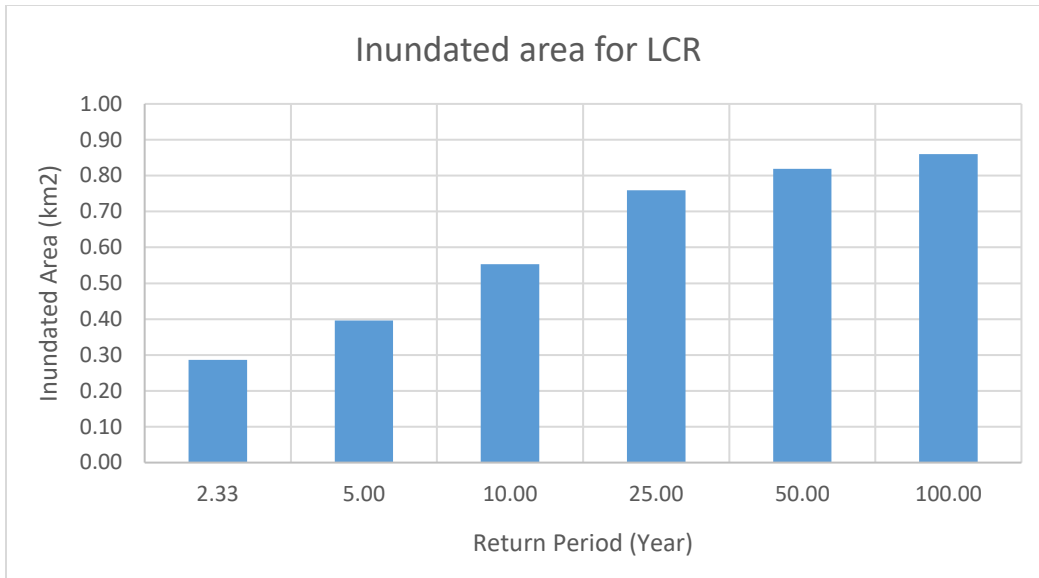
Figure 11: Inundation area for floods of different return periods.

In a depth-wise study of the inundation area (Figure 12), it was found that the depth of flooding increased with return period except for the depth class of 0-3 meter. For 50 and 100 year return periods, the area under 0-3 meter depth decreased which might be due to the topographic variation further away from the river.
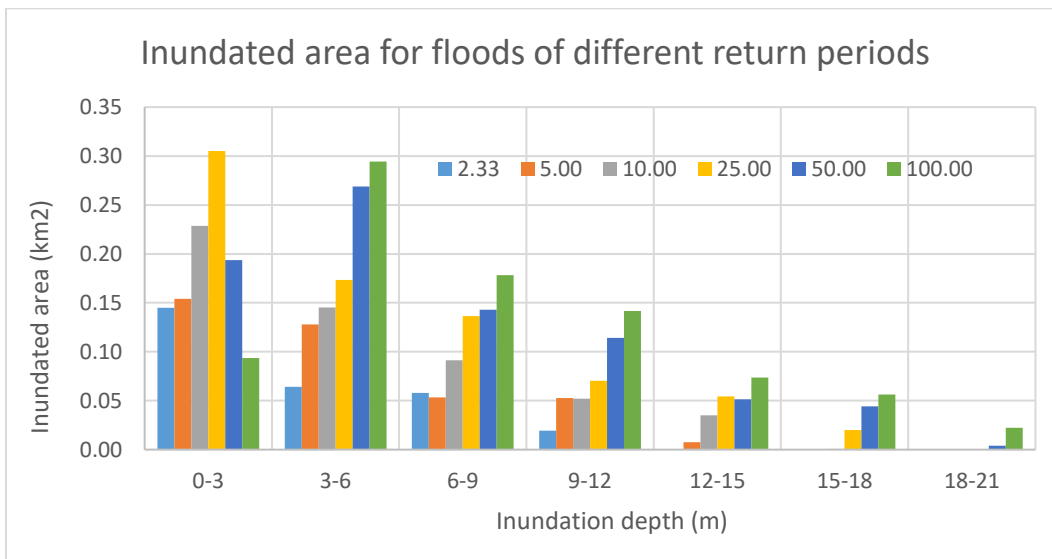
Figure 12: Depth-wise inundation area associated with flood of different return periods.

Shortcomings of the model and further study: Ineffective flow areas and obstructions on the flood plain were not digitized and hence not included in the HEC RAS analysis. Only the main river of the LCR was included in the model. There are some tributaries to the river within the study reach which need to be digitized and included into the model. Satellite image of flooding for a particular flood event, if available could be reconciled to the inundation map for a comparable flood magnitude (of a return period) produced in this analysis.

Conclusion:

The integration of HEC-RAS and GIS analysis was explored to prepare inundation map for the LCR, Texas for floods of different return periods. The inundation area increased with floods of increasing return periods. Availability of fine resolution DEM, land cover, gage discharge data, and the integration of hydraulic modeling and GIS techniques help prepare inundation maps for areas of interest. Such maps can be used to detect deficiencies in existing flood control measures and for arbitrating damage claims later. As an extension of this study, flood inundation mapping by HAND approach (Tarboton D.G., 2016) will be done and compared with the present study.

Acknowledgment:

References:

Briody, Alyse C., M. Bayani Cardenas, Pin Shuai, Peter S. K. Knappett, and Philip C. Bennett. (2016). "Groundwater flow, nutrient, and stable isotope dynamics in the parafluvial-hyporheic zone of the regulated Lower Colorado River (Texas, USA) over the course of a small flood." *Hydrogeology Journal* 24 (4): 923–35. doi:10.1007/s10040-016-1365-3.

Kalyanapu, Alfred J., Steven J. Burian, and Timothy N. McPherson. (2010). "Effect of Land Use-Based Surface Roughness on Hydrologic Model Output." *Journal of Spatial Hydrology* 9 (2). http://www.spatialhydrology.net/index.php/JOSH/article/view/84.

Merwade, Venkatesh, Aaron Cook, and Julie Coonrod. (2008). "GIS Techniques for Creating River Terrain Models for Hydrodynamic Modeling and Flood Inundation Mapping." *Environmental Modelling & Software* 23 (10–11): 1300–1311. doi:10.1016/j.envsoft.2008.03.005.

Merwade. (2016). "Tutorial on using HEC-GeoRAS with ArcGIS 10.x and HECRAS Modeling". http://web.ics.purdue.edu/~vmerwade/education/georastutorial.pdf

Salimi, Shokoufeh, M. Reza Ghanbarpour, Karim Solaimani, and Mirkhalegh Z. Ahmadi. (2008). Floodplain Mapping Using Hydraulic Simulation Model in GIS." *Journal of Applied Sciences* 8: 660–65.

Sanders, Brett F. (2007). "Evaluation of on-Line DEMs for Flood Inundation Modeling." *Advances in Water Resources* 30 (8): 1831–43. doi:10.1016/j.advwatres.2007.02.005.

Sanyal, Joy, and X. X. Lu. (2004). "Application of Remote Sensing in Flood Management with Special Reference to Monsoon Asia: A Review." *Natural Hazards* 33 (2): 283–301. doi:10.1023/B:NHAZ.0000037035.65105.95.

Tarboton D.G. (2016). HAND Flood Inundation. http://hydrology.usu.edu/dtarb/giswr/2016/

US Army Corps of Engineers. (2016). Software. http://www.hec.usace.army.mil/software/

USGS. 2014. PeakFQ: Flood Frequency Analysis. http://water.usgs.gov/software/PeakFQ/

USGS. 2016. The National Map Viewer. https://viewer.nationalmap.gov/viewer/.